

## Particle simulations of energetic particle driven Alfvén modes in JT-60U

G. Fogaccia, S. Briguglio, G. Vlad, F. Zonca, K. Shinohara<sup>†</sup>, M. Ishikawa<sup>†</sup>, M. Takechi<sup>†</sup>

*Associazione EURATOM-ENEA, CR ENEA-Frascati,*

*Via E. Fermi 45, 00044 Frascati, (Rome) Italy*

<sup>†</sup>*Japan Atomic Energy Agency, Naka, Ibaraki 311-0193, Japan*

Two different types of bursting modes, both in the frequency range of Alfvén modes, have been observed by MHD spectroscopy in auxiliary heated (NNB) discharges in the JT-60U tokamak. They have been dubbed abrupt large-amplitude events (ALEs) and, respectively, fast frequency sweeping (fast FS) modes [1]. The ALE is characterized by a time scale of the order of hundred microseconds, a relatively large fluctuating magnetic field level ( $\tilde{B}_\theta/B_\theta \sim 10^{-3}$  at the first wall) and large growth rates (corresponding to wide frequency spectra  $\Delta\omega \sim \omega \sim 50$  kHz). It is followed by a significant drop of the neutron emission rate in the central plasma region. Such a change can be attributed to a redistribution of the energetic ions, with a marked reduction of their on-axis density. The period between ALEs appears to be related with the amount of such reduction. Between two ALEs, a relatively quiescent phase is observed, characterized by a succession of several fast FS modes. Compared with ALEs, such modes show longer time scales (few milliseconds), lower growth rate and fluctuating field level, and much smaller redistribution of the energetic ions. Most of them consist of bifurcating branches, chirping up and down in frequency. Aim of the present paper is to provide a possible explanation of this phenomenology based on the investigation of the nonlinear behavior of Alfvén modes. With this scope, we perform particle simulations of a typical NNB-heated JT-60U discharge (E036378) with the HMGC code[2]. In particular, we simulate the dynamics of energetic ion interactions with Alfvén modes, assuming the radial profiles experimentally observed immediately before an ALE and postulating an anisotropic slowing-down distribution function in velocity space. We observe that the linearly unstable phase is dominated, in this "ALE" simulation, by a fast-growing mode ( $\gamma/\omega \approx 0.5$ ), located around the maximum energetic-ion pressure gradient ( $r/a \approx 0.5$ ) and characterized by a significant coupling with the Alfvén continuum, showing the energetic-particle-driven nature of the mode (Fig. 1 *left*). The saturated phase presents a complex phenomenology. At an earlier stage, the configuration is dominated by a TAE-like mode, localized around  $r/a \approx 0.8$ . The original mode, localized at half radius, is replaced by a couple of nearly degenerate modes. A weak core-localized mode also appears, with frequency well localized in the continuum gap (Fig. 1 *center*). At later times, the core-localized mode becomes the dominant one, while

the external mode still persists at lower amplitudes (Fig. 1 *right*). Figure 2 shows the contour plot in the energetic-ion ( $\hat{\mu}, \hat{v}_{\parallel}$ ) space of the wave-particle power transfer averaged over the radial annulus  $0.36 < r/a < 0.67$ , where the most unstable mode is localized, during the linear phase. Here,  $\hat{\mu}$  and  $\hat{v}_{\parallel}$  are normalized magnetic moment and parallel velocity.

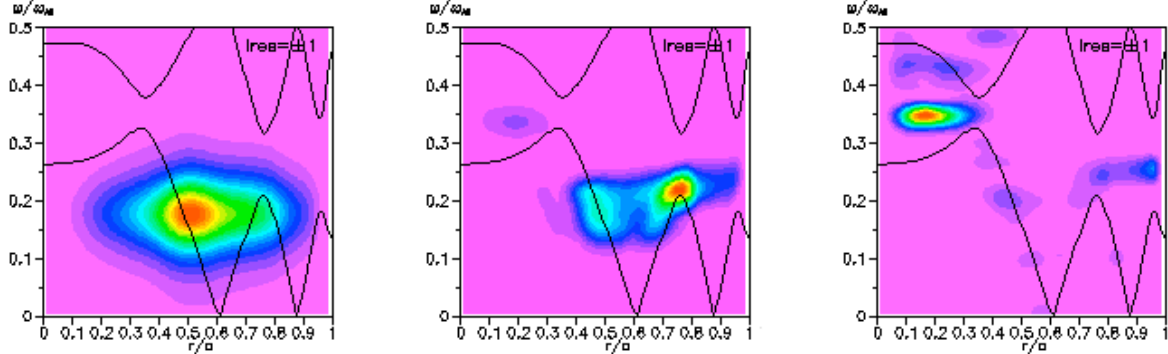


Figure 1: Contour plots of the power spectrum of the fluctuating scalar potential in the  $(r/a, \omega/\omega_{A0})$  plane, for a typical JT-60U discharge (E036378), during the linear-growth phase (*left*) and the earlier (*center*) and later (*right*) saturated phases. The Alfvén continuum spectrum is also plotted by the black line. Here,  $\omega_{A0}$  is the on-axis Alfvén frequency.

The continuous and dashed lines correspond to trapped-to-circulating particle transition at the boundaries of the annulus; the dotted line indicates the injection energy of the beam ions. We see that the resonant drive is given by circulating energetic ions, consistently with the nearly tangential beam injection. The resonance region appears to be quite broad in energy, in agreement with the experimental observations [3]. As the nonlinear effects become important, a macroscopic outward displacement of the energetic particles is observed, producing a significant reduction of their density in the central region (Fig. 3 *left*).

Given the fair agreement between numerical results and experimental observations, we investigate whether the nonlinear dynamics described by our simulations can also explain the relatively quiescent phase (low amplitude fluctuating fields with negligible effects on the energetic-ion distribution) between two successive ALEs. As a first step, we check to which extent the reduced instability level of the system after an ALE is due to the weaker drive associated with the reduction of the energetic-ion density radial gradient. Thus, we perform a simulation ("after ALE"), analogous to the previous one, but

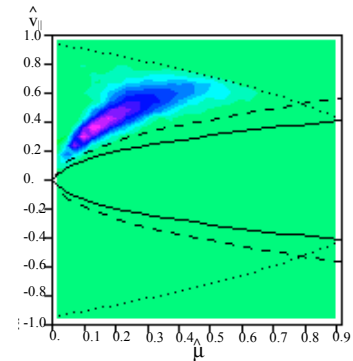


Figure 2: Contour plot in the energetic-ion ( $\hat{\mu}, \hat{v}_{\parallel}$ ) space of the wave-particle power transfer averaged over the radial annulus  $0.36 < r/a < 0.67$ , during the linear phase.

with initial energetic-ion density profile equal to that experimentally observed after the ALE. The results we obtain show that, in spite of fairly little nonlinear effects on the spatial energetic-ion distribution (Fig. 3 *center*), the fluctuating field levels are quite large: approximately half of the values found in the "ALE" simulation, to be compared with the experimental observation for the fast FS-to-ALE amplitude ratio ( $\sim 0.2$ ). This seems to be inconsistent with the observed

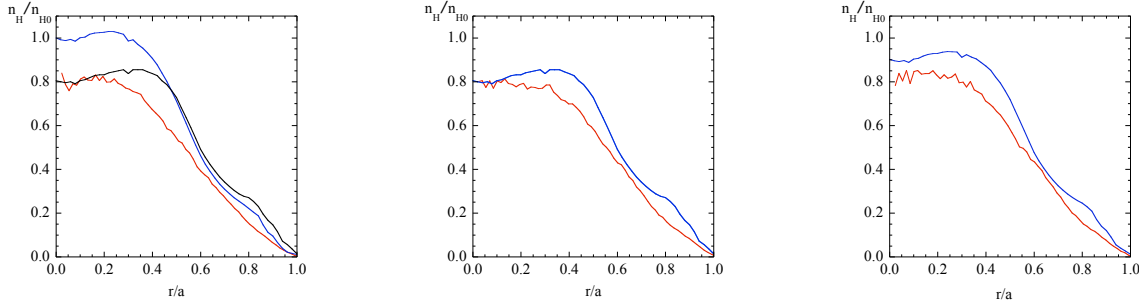


Figure 3: Nonlinear modifications of the energetic ion density profile yielded by the three simulations: "ALE" (*left*), "after ALE" (*center*) and "intermediate" (*right*). Blue curves refer to the initial profiles; red curves, to the simulation relaxed profiles; the black curve in the *left* frame shows the experimentally observed profile just after the ALE .

periodic character of the ALEs: with such a level of instability, even a partial reconstruction of the spatial energetic-ion density profile would generate a fast instability, which would essentially clamp the energetic-ion density profile to the "after-ALE" shape. This is confirmed by a third simulation ("intermediate"), characterized by an intermediate initial energetic-ion density profile: the final profile is substantially coincident with that found at the end of the two previous simulations (Fig. 3 *right*).

This apparent contrast between numerical results and experimental observations can be reconciled accounting for the fact that, differently from what we assumed in the latter simulations, the velocity-space distribution function after an ALE is not a slowing-down. In other words, retaining only part of the ALE nonlinear effects (the spatial redistribution), with no attention to the distortion produced in the velocity space, is not sufficient.

To show this, we perform a further numerical experiment ("after ALE modified"), by prolonging the original "ALE" simulation artificially suppressing the fluctuating fields immediately after the saturation of the dominant mode has been reached. In this way, the evolution of the system after the first relaxation of the energetic-ion density profile takes into account both the velocity-space distortion produced by the large amplitude event and the observed damping of the fields after the ALE. Figure 4 *left* shows the numerical time trace of fluctuating poloidal magnetic field close to the wall for such simulation (blue curve). The mode we identified as

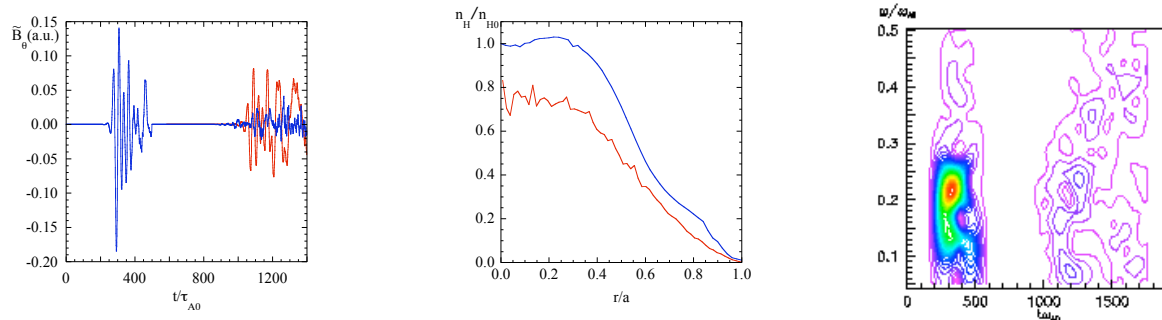


Figure 4: "After ALE modified" simulation. Left: fluctuating poloidal magnetic field, close to the wall, versus time (blue curve); the results obtained in the "after ALE" simulation are also reported (red curve). Center: initial (blue curve) and relaxed (red curve) energetic-ion density profile. Right: power spectrum of the fluctuating poloidal magnetic field in the  $(t, \omega)$  plane.

an ALE is observed at  $t \sim 300\tau_{A0}$ , with  $\tau_{A0} \equiv \omega_{A0}^{-1}$  being the Alfvén time; the weaker mode, at  $t \sim 1200\tau_{A0}$ . Note that the time interval between the two bursts depends on the simulation details (e.g., the "suppressed" fluctuating field level): it is not directly related with the time separation of bursting modes in the experiments. We see that the fluctuating field level of the latter mode is now lower than the value found, without taking into account the redistribution in the velocity space, in the "after ALE" simulation (superimposed, for comparison, in the same Figure: red curve). The global effect on the energetic-ion density profile is shown in Fig. 4 center. Finally, the power spectrum of the fluctuating poloidal magnetic field close to the wall in the  $(t, \omega)$  plane is reported in Fig. 4 right: the frequency sweeping of the weaker fluctuation supports its identification with a fast FS mode.

On the basis of these results, a possible interpretation of the experimental observations could be the following: given the energetic-ion source provided by the beam injection, the free energy reconstruction rate is set by the need of rebuilding the velocity space distribution function. In this way, the intermediate configurations between two successive ALEs are characterized by a lower drive than that of a slowing-down distribution with the same energetic-ion density profile. Low growth rates and amplitude modes, such as the fast FS modes, are then excited and have a weaker effect than that of ALEs in contrasting the density profile reconstruction. As soon as the combined restoration of the configuration and velocity space distribution provides enough drive for a fast growing Alfvén mode, a new ALE occurs.

## References

- [1] Shinohara K. et al. 2001 *Nucl. Fusion* **41** 603–612.
- [2] S. Briguglio, G. Vlad, F. Zonca and C. Kar, *Phys. Plasmas*, **2** (1995) 3711.
- [3] Ishikawa M. et al. 2005 *Nucl. Fusion* **45** 1474–1480.